

Published in final edited form as:

J Neurosci. 2010 April 14; 30(15): 5334–5345. doi:10.1523/JNEUROSCI.5963-09.2010.

***Dlx5* and *Dlx6* Regulate the Development of Parvalbumin-Expressing Cortical Interneurons**

Yanling Wang^{1,+,*}, Catherine A. Dye^{1,2,+}, Vikaas Sohal⁷, Jason E. Long^{1,3}, Rosanne C. Estrada⁴, Tomas Roztocil⁵, Thomas Lufkin⁶, Karl Deisseroth⁷, Scott C. Baraban⁴, and John L.R. Rubenstein^{1,*}

¹Department of Psychiatry, Nina Ireland Laboratory of Developmental Neurobiology, University of California, San Francisco, 1550 4th street, San Francisco, CA 94158, USA ²Department of Psychology, University of California, Riverside, Riverside, CA ³Genentech Corp., South San Francisco, CA ⁴Epilepsy Research Laboratory, Department of Neurological Surgery, University of California, San Francisco, CA ⁵Merck Serono, Geneva, Switzerland ⁶Genome Institute of Singapore, 60 Biopolis Street, Singapore 138672 ⁷Departments of Psychiatry and Bioengineering, Stanford University, Stanford, CA

Abstract

Dlx5 and *Dlx6* homeobox genes are expressed in developing and mature cortical interneurons. Simultaneous deletion of *Dlx5* and *6* results in exencephaly of the anterior brain; despite this defect, prenatal basal ganglia differentiation appeared largely intact, while tangential migration of *Lhx6*⁺ and *Mafb*⁺ interneurons to the cortex was reduced and disordered. The migration deficits were associated with reduced *CXCR4* expression. Transplantation of mutant immature interneurons into a wild type brain demonstrated that loss of either *Dlx5*, or *Dlx5&6*, preferentially reduced the number of mature parvalbumin⁺ interneurons; those parvalbumin⁺ interneurons that were present had increased dendritic branching. *Dlx5/6*^{+/-} mice, which appear normal histologically, show spontaneous electrographic seizures, and reduced power of gamma oscillations. Thus, *Dlx5&6* appeared to be required for development and function of somal innervating (parvalbumin⁺) neocortical interneurons. This contrasts with *Dlx1*, whose function is required for dendrite innervating (calretinin⁺, somatostatin⁺ and neuropeptide Y⁺) interneurons (Cobos et al., 2005).

Keywords

Dlx5; *Dlx6*; Cortical Interneuron; Parvalbumin; Transplantation; Subtype Specification

Introduction

Most rodent cortical interneurons are derived from progenitor domains in the prenatal subcortical telencephalon (subpallium) (Marin et al., 2003; Flames and Marin, 2005). The subpallium consists of four major subdivisions that have distinct molecular and morphological features: the lateral ganglionic eminence (LGE), medial ganglionic eminence

*Correspondence: Yanling.wang@ucsf.edu (Y.W), john.rubenstein@ucsf.edu (J.L.R.R.).

+Co-first authors

The authors contributed to the following figures: Figs.1, 4: YW, CD, JL; Figs. 2, 3, 5, 6, 7: YW; Fig.8: YW, VSS, SCB, RCE; Supplemental Fig.1: YW, CD; Supplemental Figs 2, 3, 7: CD, TR, JL; Supplemental Figs. 4, 5, 6, 8, 9, 10,11: YW.

(MGE), septum (SE) and preoptic area (POA). Moreover, caudal ganglionic eminence (CGE) exists as a caudal fusion of the MGE and LGE with distinct molecular domains that resemble caudal extensions of the MGE and LGE (Long et al., 2007).

The MGE is the source of the majority of interneurons that express parvalbumin (PV) and somatostatin (SST). On the other hand, there are at least two types of calretinin⁺ and neuropeptide Y (NPY)⁺ interneurons: those expressing somatostatin are thought to derive from the MGE, and those that don't express somatostatin are thought to mainly derive from the CGE (Sussel et al., 1999; Pleasure et al., 2000; Xu et al., 2004; Butt et al., 2005; Wonders and Anderson, 2006; Flames et al., 2007; Fogarty et al., 2007; Xu et al., 2008). Flames et al. (2007) found that dorsal and ventral subdivisions of the MGE produce different ratios of cortical interneuron subtypes; dorsal regions preferentially produce SST⁺, whereas ventral regions preferentially produce PV⁺. They correlated this with molecular features of the MGE to provide insights for a transcription factor code in generating distinct neocortical interneuron subtypes.

Information about the transcriptional control of interneuron development has come from the analysis of *Arx*, *Dlx1&2*, *Dlx1*, *Lhx6*, and *Nkx2.1* mutants. Most interneurons require *Dlx1&2* (Anderson et al., 1997a; Anderson et al., 1997b; Yun et al., 2002; Cobos et al., 2006; Long et al., 2007) Long et al., 2009a,b). *Dlx1/2*^{-/-} mutants have a severe deficit in the survival and migration of immature cortical and hippocampal interneurons. While *Dlx1* is widely expressed in immature interneurons, its postnatal expression is only detectable in subsets of SST⁺, NPY⁺ and most CR⁺ interneurons, where it is required for their survival (Cobos et al., 2005; Cobos et al., 2006; Cobos et al., 2007). Virtually all PV⁺ and SST⁺ interneurons, and subsets of CR⁺ and NPY⁺ interneurons, depend on expression of *Nkx2.1* and *Lhx6* (Sussel et al., 1999; Pleasure et al., 2000; Liodis et al., 2007; Du et al., 2008; Zhao et al., 2008). *Dlx1/2*^{-/-} and *Lhx6*^{-/-} have reduced *Arx* expression. (Cobos et al., 2006; Zhao et al., 2008). *Arx* mutants have reduced interneuron migration (Kitamura et al., 2002; Colasante et al., 2008) (Colombo et al., 2007; Fulp et al., 2008). While the function of *Dlx1* and *Dlx2* in telencephalic development has been well established, the function of *Dlx5* and *Dlx6* is just beginning to be elucidated. *Dlx5* is known to promote differentiation of olfactory bulb interneurons (Levi et al., 2003; Long et al., 2003); no information is available on *Dlx6* function. Because *Dlx1&2* are required to induce expression of *Dlx5&6* in the LGE and MGE subventricular zones (Anderson et al., 1997a; Zerucha et al., 2000; Long et al., 2007), it is unclear to what extent the *Dlx1/2*^{-/-} phenotype reflects loss of *Dlx1&2* or *Dlx1,2,5&6* function. Here we present the first evidence that *Dlx5* and *Dlx5&6* are required for development and function of neocortical PV⁺ interneurons.

Materials and Methods

Animals and tissue preparation

Dlx5 and *Dlx5&6* loss of function mutant mice were previously described (Depew et al., 1999; Robledo et al., 2002). *Lhx6*-GFP and *Dlx5*-GFP BAC transgenic mouse line were obtained from GENSAT (<http://www.gensat.org/index.html>). *Dlx5/6i-Cre* mice were also previously described (Kohwi et al., 2007). For staging of embryos, midday of the vaginal plug was calculated as embryonic day 0.5 (E0.5). Mouse colonies were maintained in accordance with the protocols approved by the Committee on Animal Research at University of California, San Francisco. Embryos were anesthetized by cooling, dissected, and immersion fixed in 4% paraformaldehyde (PFA) in PBS for 4–12 h. Samples were then cryoprotected in 30% sucrose and cut 20um using a cryostat.

***In situ* hybridization**

In situ hybridization experiments were performed using digoxigenin riboprobes on 20 μm frozen sections as described previously. Briefly, slides were fixed in 4% PFA for 20 min, treated with proteinase K (1 $\mu\text{g}/\text{ml}$) for 15 min. Acetylation was performed using 0.25% acetic anhydride in 0.1 M triethanolamine, pH 8.0, for 10 min, followed by three PBS washes. Slides were incubated with hybridization buffer for 2 hours at RT, followed by overnight incubation with a digoxigenin-labeled probe at 72°C. Three high-stringency washes were performed with 0.2 \times SSC at 72°C. Slides were then incubated with horseradish alkaline phosphatase -conjugated anti-digoxigenin and NBT (nitroblue tetrazolium)/BCIP (5-bromo-4-chloro-indolyl phosphate) for signal detection. The probes used and their sources were as follows: *Cxcl12* (Sam Pleasure), *Cxcr4* (Dan Littman), *Cxcr7* (RDC1) (ATCC MGC-18378), *Dlx1*, *Dlx2* (J.L.R.R.'s laboratory), *ErbB4* (Cary Lai), *Gad67* (Brian Condie), *Gucy1a3* (Imagen/Gene Cube), *Ikaros* (Katia Georgopolos), *Lhx6* (Vassilis Pachnis), *Reelin* (Tom Curran), *RXR γ* (Kenny Campbell) *Somatostatin* (Tom Lufkin), *Tiam2* (BM228957) and *VGAT* (NM_009508.2).

Immunohistochemistry

Animals were deeply anesthetized (P60) and perfused intracardially with 4% paraformaldehyde in phosphate-buffered solution (PB 0.1 M, pH 7.4). The brains were removed and postfixed overnight in the same fixative and cryoprotected by immersion in 30% sucrose. Free-floating cryostat sections (40 μm) were processed using standard procedures. Primary antibody dilutions used were as follows: rabbit anti-calretinin (CR) (1:2000, Immunostar) anti-Parvalbumin (1:2000; Swant Swiss Abs),; rat anti-Somatostatin (1:200, Chemicon) or rabbit anti-NPY (1:2000, Immunostar), rabbit anti-GFP (1:2000, Molecular Probes), anti-Phosphorylated Histone H3 (1:200, Upstate). Secondary antibodies were as follows: Alexa 488 goat anti-rabbit, Alexa 488 goat anti-chicken, Alexa 594 goat anti-rat, Alexa 594 goat anti-rabbit. Immunoperoxidase staining was performed by using the ABC elite or M.O.M. kit (Vector, Burlingame, CA).

MGE dissections

Exencephalic telencephali of *Dlx5/6*^{-/-} mutants possess a characteristic appearance, the pallium is located laterally, whereas the subpallium is located in medially (supplemental Fig. 1A, 1B, 1C, 1D). To gain a better view of GFP expression in *Dlx5/6*^{-/-} brains, we removed the pallium from the subpallium and positioned (flipped) the subpallium so that its pial side faced upwards (supplemental Fig. 1G). The area with the strongest GFP intensity in *Dlx5/6*^{-/-} mutants was located slightly off of the medial-most side of the telencephalon, roughly half way along the rostral-caudal axis, and deep to the ventricular surface. This intensely positive GFP region was present in all genotypes studied: *Dlx5*^{+/+}, *Dlx5*^{-/-}, *Dlx5/6*^{+/+} and *Dlx5/6*^{-/-}, and was designated the MGE mantle zone (MZ)/ventral subpallium (Supplemental Fig. 1E & 1F). For transplantation, we used the VZ/SVZ region just superficial to the intensely GFP positive region. To dissect the VZ/SVZ region of *Dlx5/6*^{-/-} MGE, four cuts were made at the edges of the intensely GFP positive region; two cuts were made along medial-lateral axis at their anterior and posterior limits, then two were made along the rostral-caudal axis at their lateral and medial limits (Supplemental Fig. 1G). The excised tissue block corresponds to the MGE; it was then rotated 90 degrees, placing it on one of its cutting surfaces. We then made an incision that separated the VZ/SVZ from the MZ. The surface VZ/SVZ region (dotted line area in Supplemental Fig. 1E & 1F) was removed and processed for the transplantation and cell culture.

Transplantation

Cell transplantations of interneuron precursors from *Dlx5*^{+/+}, *Dlx5*^{-/-}, *Dlx5/6*^{+/+} and *Dlx5/6*^{-/-} donors into WT neonates (P0) were performed as described previously (Cobos et al., 2005). Embryos carrying Lhx6-GFP BAC transgene were dissected at E13.5. VZ/SVZ regions of medial ganglionic eminences were dissected from each embryo in HBSS (Gibco). Explants were then washed with 200ul of HBSS medium containing 50 ug/ml DNase I (Roche, Indianapolis, IN) and mechanically dissociated. Dissociated cells were concentrated by centrifugation (3 minutes, 800 g) and resuspended in 2 ul of HBSS. Cell suspensions were loaded into glass micropipettes (~50 um diameter) that were pre-filled with mineral oil. Micropipettes were connected to a microdispenser (Drummond) with direct readout for fractional microliters. Recipient pups (P0) were anesthetized on ice. A total of 5×10^5 cells per mouse in a 100–200 nl volume was injected into parietal cortex in a single point using a 45° inclination angle. Grafted pups were returned to their mothers and analyzed after 2 months. The percentage of GFP+ cells expressing CR, PV, SST or NPY in grafted animals was determined using a BX-60 microscope (Olympus, Melville, NY) equipped with epifluorescence illumination. At least 100 GFP+ in cortex were analyzed per each marker in each animal.

Cell culture

Cultures of *Dlx5/6*^{+/+} or ^{-/-} MGE cells were established and maintained using previously described methods (Xu et al., 2004). Briefly, the MGE was identified by both morphological appearance and by location of GFP fluorescence, and dissected into cold Hank's Buffer. Tissue was cut into pieces and transferred into Neurobasal medium supplemented with B-27 prior to trypsinization. Trypsinization for 15' at 0.05% + 10ug/ml DNase was carried out at 37°C, terminated by the addition of an excess of DMEM supplemented with Fetal Bovine Serum (FBS), and followed by two rounds of mechanical dissociation. The first used large bore Pasteur pipettes, the second used small bore pipettes. Cells were pelleted in between and following the second dissociation by centrifugation at 2000 rpm, 4°C, 4 min, and resuspended in cold DMEM/FBS. Prior to plating, cells were strained and counted using a hemocytometer. 5000 MGE cells were plated into one chamber (0.4cm²) of a 16 chamber slide (LABTEK) that had been previously coated with laminin and poly-L-lysine (2 days prior) and seeded (1 day prior) with approximately 1×10^5 cortical cells isolated from GFP-negative CD1 P0 or P1 neonates as described above. Cultures were grown at 37°C under 5-6% CO₂. 50% of the media was exchanged for NB/B-27 at 1 day post plating, 2 days post plating, and every other day following. At the termination point, cells were fixed in 4% Paraformaldehyde/PBS prior to GFP immunohistochemistry. GFP cells were counted by hand using a compound fluorescence microscope. The ratio of the numbers of GFP positive cells/chamber at 5 days *in vitro* (DIV) and 10DIV or 5DIV and 40 DIV is defined as Percent Survival.

Video- electroencephalography (EEG)

For monitoring, surface head mount EEG hardware was purchased from Pinnacle Technology, Inc. (Lawrence, KS). Mice were anesthetized and the skull surface was exposed with a single rostral/caudal incision. Head mounts were attached with four conductive stainless steel screws, which also acted as recording electrodes. Two wires were laid on top of the shoulder muscles for electromyographic recording. Dental cement was used to secure the head mount, and mice recovered for four days before recordings commenced. Recordings were sampled at 400 Hz and high-pass filtered at 1 Hz (EEG) and 10 Hz (EMG). Each mouse was monitored 3-12 hours/day; up to 8 non-consecutive days (alternating day and night recording sessions when possible). A total of 16,980 min (34 d) of recording were obtained for *Dlx5/6*^{+/+} mice and 9,933 min (28 d) for controls. Low-pass filtering was done at 40 Hz (EEG) and 100 Hz (EMG). Simultaneous video was obtained at

two different angles using Microsoft LifeCam VX-3000 cameras linked via a USB-port to a PC-based computer running Active WebCam software. Seizure discharges were detected by SireniaScore software (Pinnacle) and confirmed by off-line review by an investigator blind to the status of the animal.

Wavelet-based power measurements

We measured power in 60-second EEG recordings. We recorded EEG from two sites in each mouse, as described previously (Baraban et al., 2009). Recordings were chosen to occur during period of wakefulness and to be free of cortical spikes and electrographic seizures. For each 60-second recording, we computed the power as a function of frequency and time. Frequency varied between 4 and 200 Hz, using 2 Hz increments. Time was measured by dividing each 60-second recording into 1-second epochs. To measure the power at frequency f within each 1-second long epoch, we first bandpass filtered the recording between $f \pm 2$ Hz, then convolved the filtered signal with a wavelet with frequency f , defined as: $Wf = e^{-t^2/43f^2} e^{2\pi i f t}$.

We used the squared amplitude of the result to measure the instantaneous power at that frequency. The power during a 60-second recording was the average of the power measured during each of the 1 second long epochs within that recording.

Cell counting in histological sections

The number of interneurons expressing different genes (E16.5), the percentage of *Dlx5*-*GFP*⁺ cells expressing DLX2 (E15.5) or standard interneuron markers (P60), were determined in the lateral cortex (E15.5 & E16.5) and somatosensory cortex (P60) respectively. Statistical analysis was performed using the Student's *t*-test or ANOVA analysis.

Results

Exencephalic *Dlx5/6*^{-/-} mutants have normal telencephalic patterning

Previous reports demonstrated that simultaneous deletion of *Dlx5* and *6* results in exencephaly in the anterior brain, which is mainly due to distinctive craniofacial defects and the complete absence of calvaria. (Depew et al., 2002; Robledo et al., 2002). To evaluate regional patterning and differentiation within this dysmorphic forebrain, we used *in situ* hybridization on E15.5 coronal sections. As a visual aid, we show schematic representations of the pallial and subpallial domains of coronal sections of wild type and *Dlx5/6*^{-/-} (Fig. 1S&1T, Supplemental Fig. 2). *Dlx1* and *Dlx2* are expressed in the subpallial VZ and SVZ (ventricular and subventricular zones), and in migratory interneurons on their path from the MGE and caudal LGE into the cortex (Fig. 1A & C); their expression appeared intact in the VZ and SVZ of the LGE and MGE (Fig. 1B & 1D), and in interneurons that are tangentially migrating to the cortex (see Fig. 4 for higher magnification). *Lhx6* labels the SVZ and the mantle region of the MGE, and a large fraction of tangentially migrating interneurons; this expression was largely preserved in the *Dlx5/6*^{-/-} mutants (Fig. 1E & 1F, Supplemental Fig. 3; see Fig. 4 for higher magnification).

In *Dlx1/2*^{-/-} mutants, *Dlx5* and *6* expression are almost eliminated from the LGE and MGE (Anderson et al., 1997b); thus it is possible that a significant component of their phenotype results from the loss of *Dlx5* and *6* expression. Thus, we assessed the expression of a subset of genes that are strongly down-regulated in the LGE and MGE of *Dlx1/2*^{-/-} mutants (*VGAT*, *CXCR7*, *Tiam2*, *Gucy1a3*, *RXRγ* and *Ikaros*) (Long et al., 2007; Long et al., 2009a; Long et al., 2009b). However, in the *Dlx5/6*^{-/-} mutants, expression of these genes was not grossly

reduced (Fig. 1G-1R), demonstrating that their transcription is strongly dependent on *Dlx1* & 2 or other downstream effectors.

Interneuron migration is reduced in *Dlx5/6*^{-/-} mutants

The majority of GABAergic interneurons of neocortex and hippocampus are generated from the ganglionic eminences and tangentially migrate to the developing cortex. Early-born populations of interneurons emerge from the MGE and invade the cortex by E13. To examine if the *Dlx5/6*^{-/-} mutation affects early interneuron migration, we assessed expression of interneuron markers (*Dlx1*, *Lhx6* and *somatostatin*) by *in situ* hybridization. In *Dlx5/6*^{+/+} embryos, superficial and deep migratory streams were present in the MZ and IZ/SVZ, respectively, and the leading migrating cells (denoted by black arrows) in MZ already reached the dorsal cortex (Fig2A, 2E, 2I). In *Dlx5/6*^{-/-} embryos, the leading migrating cells did not migrate as far into the dorsal neocortex as in wild type controls (black arrows in Fig2C, 2G, 2K); Although the deep migratory stream was maintained, the superficial migratory stream was poorly formed (black arrowheads in Fig2D, 2H, 2L compared with those in Fig. 2B, 2F, 2J).

To follow the progression of this phenotype, we studied the interneuron distribution using a transgenic marker. We crossed a BAC transgene encoding the *Lhx6* gene, which is driving expression of green fluorescent protein (GFP) (Cobos et al., 2006). GFP immunohistochemistry in *Dlx5/6*^{+/+} and *Dlx5/6*^{-/-} telencephalons at E12.5, E13.5 and E14.5 revealed a progressive retardation in the migration of *Lhx6*-expressing interneurons, in both the deep and superficial migratory streams in *Dlx5/6*^{-/-} mutants (Fig. 3). We noticed that leading migrating cells in *Dlx5/6*^{-/-} mutants at E14.5 reached roughly half way as far as that in *Dlx5/6*^{+/+} controls. This evidence for a delay suggested that all *Lhx6*-GFP⁺ interneurons (may include some interneurons that don't normally express *Dlx5/6*) were affected upon loss of *Dlx5/6* function. It should be noted that we can not rule out that the exencephalic phenotype contributed in a non-autonomous manner to this phenotype. We also detected an accumulation of *Lhx6*⁺ interneurons in the SVZ of lateral ganglionic eminences (supplemental Fig. 4), suggesting reduced efficiency in the tangential migration of interneurons in *Dlx5/6*^{-/-} mutants. Overall, *Dlx5/6*^{-/-} mutants demonstrated a slowing of migration rather than a block in migration, in contrast with the *Dlx1/2*^{-/-} mutants (Anderson et al., 1997a; Marin et al., 2000).

The exencephalic *Dlx5/6*^{-/-} brains underwent degeneration at late gestational stages; the oldest brains that we could reliably analyze were E16.5. At this stage, we assessed neocortical interneuron molecular properties and extent of their migration by performing *in situ* hybridization to detect *Dlx1*, *Dlx2*, *GAD67*, *Lhx6*, and *MafB* (Fig. 4A-L). We quantified the total number of cells expressing these genes within 125,000μm² of the lateral cortex, and the number of positive cells in each of the cortical layers (VZ, SVZ, IZ, CP, MZ). Our data showed that there was a general reduction of *Dlx1*⁺, *Dlx2*⁺, *GAD67*⁺, *Lhx6*⁺ cells in lateral cortex; the reduction was most severe in MZ and SVZ, however there was a preferential depletion of *Lhx6* and *MafB* within the MZ (see histograms in Fig. 4M). Furthermore, while the number of *MafB*⁺ cells was normal, their laminar distribution was greatly disturbed (Fig. 4M). Thus, the *Dlx5/6*^{-/-} mutation appears to preferentially affect the *Lhx6*⁺ and *MafB*⁺ migrating interneurons within the neocortex.

Loss of *CXCR4* expression in deep migrating interneurons in the *Dlx5/6*^{-/-} mutants

Towards elucidating the mechanism(s) underlying the reduced number of interneurons in the *Dlx5/6*^{-/-} cortex, we tested the expression of molecules that are implicated in regulating interneuron migration. To determine whether the exencephaly altered the properties of the meninges, we examined expression of the cytokine stromal-derived factor-1 (SDF1), which

is known to regulate migration and laminar positioning of interneurons and Cajal Retzius cells (Stumm et al., 2003; Borrell and Marin, 2006; Li et al., 2008; Lopez-Bendito et al., 2008). Despite the gross malformation, *SDF1* expression in the meninges was apparent; however, the cavity formed by the everted exencephalic cortex was filled with *SDF1*⁺ cells. (* in Fig.5B'). *SDF1* expression in the intermediate zone of ventro-lateral cortex appeared normal (Fig. 5B & 5B').

Next we assessed the properties of the neocortical marginal zone, which contains *Reelin*-expressing Cajal Retzius cells that tangentially migrate over its surface from several sources (Bielle et al., 2005). *Reelin* expression has a prominent role in regulating the laminar position of cortical projection neurons and interneurons, although it is unclear whether the interneuron phenotypes are cell autonomous (Hevner et al., 2004; Hammond et al., 2006; Pla et al., 2006; Yabut et al., 2007). *Reelin* expression appeared roughly normal in the *Dlx5/6*^{-/-} mutants (Fig. 5D, 5D'). Thus the tangential migration of *Reelin*⁺ cells to cover the cortex shows that the reduction of *Dlx1*, *Dlx2*, *Lhx6* and *GAD67* expression in the marginal zone is not due to a general disruption of migration in this layer.

Migrating interneurons express several known receptors that promote their migrations. First we examined expression of two receptors for *SDF1*: *CXCR4* and *CXCR7* (*RDC*, *CMKOR1*). *CXCR4* regulates laminar positioning of interneurons (Stumm et al., 2003; Li et al., 2008; Liapi et al., 2008; Lopez-Bendito et al., 2008; Tiveron and Cremer, 2008); the function of *CXCR7* has not been established, but its expression is reduced in *Dlx1/2*^{-/-} mutants (Long et al., 2009a,b). In *Dlx5/6*^{-/-} mutants, although *CXCR4* expression appeared intact in Cajal Retzius cells and in the striatum, its expression was not detectable in interneurons tangentially migrating in the cortex (arrows in Fig. 5I', 5J'). In contrast, *CXCR7* expression in migrating interneurons appeared normal (arrows in Fig. 5E', 5F').

Finally, we examined expression of *ErbB4*, a receptor for neuregulin, which also promotes interneuron migration (Flames and Marin, 2005). The expression of *ErbB4* was maintained in the MGE and LGE, and in deep migrating interneurons in *Dlx5/6*^{-/-} mutants (Fig.5G', 5H'). Furthermore, the expression of two ErbB4 ligands, neuregulin1 (NRG-1) and sensory and motor neuron-derived factor (SMDF; a form of neuregulin1) was intact in *Dlx5/6*^{-/-} mutants (Supplemental Fig. 5). Thus, the reduction in *CXCR4* expression may contribute to the interneuron migration deficit of *Dlx5/6*^{-/-} mutants.

***Dlx5/6* regulate interneuron specification in cell-autonomous manner**

While loss of *CXCR4* expression in migrating interneurons may contribute to the reduced numbers of tangentially migrating interneurons, we could not rule out the contribution of the exencephalic nature of the *Dlx5/6*^{-/-} brain. To circumvent this caveat, we transplanted E13.5 *Dlx5/6*^{-/-} mutant MGE cells into a wild type postnatal day 0 (P0) cortex. We used the *Lhx6*-BAC GFP transgene (which has previously been shown to label approximately 75-85% of PV⁺ and 55-70% of SST⁺ interneurons) (Cobos et al., 2006) as a reporter to follow the fate of MGE-derived offspring cells. Furthermore, to determine the individual role of *Dlx5* in cortical interneuron development, we performed the transplantation using MGE cells from *Dlx5*^{-/-} mutants (Long et al., 2003).

We analyzed the grafted cells at 1 and 2 months after transplantation. Of the 86 transplantations, 62 pups contained grafted cells, judged by GFP immunohistochemistry. Grafted interneuron precursors from *Dlx5/6*^{-/-} and *Dlx5*^{-/-} mutants were able to migrate, with leading migrating cells 4.0mm away from the injection site along the rostral-caudal axis, and no differences were detected in the distribution of GFP⁺ neurons between wild type, *Dlx5*^{-/-} and *Dlx5/6*^{-/-} mutants (Supplemental Fig.6). This shows that the intracortical migration of *Lhx6*-GFP⁺ interneurons (at least postnatally) may not rely on *Dlx5/6* function.

Next, we compared the percentage of neurons that differentiated into PV⁺, SST⁺, NPY⁺ and calretinin⁺ cells from the *Dlx5/6*^{+/+}, *Dlx5*^{-/-} and *Dlx5/6*^{-/-} transplants (Fig. 6A~6D). We only detected a phenotype for PV⁺ interneurons. There was a ~2-fold reduction in *Dlx5*^{-/-} transplants and a ~3 fold reduction in the *Dlx5/6*^{-/-} transplants (Fig. 6E) (*Dlx5/6*^{+/+}: 25.21±3.49%; *Dlx5*^{-/-}: 13.29±1.38%; *Dlx5/6*^{-/-}: 8.27±1.37%; *P* = 0.01).

Finally, to assess whether the *Dlx5*^{-/-} and *Dlx5/6*^{-/-} mutations affected the dendritic morphology of PV⁺ grafted cells, we studied confocal images using Image J software. Dendritic arborization of the grafted (GFP⁺) PV⁺ cells could be assessed in isolated interneurons (Fig. 6F, 6F'); we manually traced the dendritic arbors of 15 cells from each genotype and measured the number of processes, total dendritic length, average dendritic length, and longest dendrite (Fig. 6G). The *Dlx5/6*^{-/-} mutant cells showed a statistically significant increase in the number of processes compared with cells from *Dlx5/6*^{+/+} and *Dlx5*^{-/-} donors (*Dlx5/6*^{+/+}: 10.00±0.71%; *Dlx5*^{-/-}: 9.67±0.25%; *Dlx5/6*^{-/-}: 19.33±0.71%; *P* = 0.01) (Fig. 6H). Accordingly, PV⁺ cells from *Dlx5/6*^{-/-} tended to display an increase in total dendritic length (Fig. 6I). However, average dendritic length, length of the longest dendrite of PV⁺ cells from *Dlx5/6*^{-/-} decreased by the approximately 25% and 35% respectively (Fig. 6J, 6K). Dendritic morphology of *Dlx5*^{-/-} mutants was only mildly affected.

***Dlx5/6* are not essential for short-term *in vitro* cell survival of MGE cultures**

The reduced numbers of cortical interneurons in the embryonic *Dlx5/6*^{-/-} mutants, and the reduced fraction of PV⁺ interneurons transplanted from the MGE of *Dlx5/6*^{-/-} could be due to reduced survival of these cells. *Dlx1* and *Dlx2* are known to promote neuronal survival. For instance, *Dlx1*^{-/-} mutants have increased cell death of subsets of postnatal cortical interneurons, and *Dlx1&2*^{-/-} mutants have massive prenatal cell death *in vivo* in the basal ganglia and *in vitro* in cultures derived from the MGE of *Dlx1/2*^{-/-} mutants (Cobos et al., 2007). Note that loss of *Dlx1&2* expression in the MGE results in loss of *Dlx5&6* expression (Anderson et al., 1997b). Thus, to test whether MGE-derived cells of *Dlx5/6*^{-/-} mutants have reduced survival, we used the *in vitro* culture assay described in Cobos et al (2007). Unlike the *Dlx1/2*^{-/-} mutants, which have >95% cell death after 10 days *in vitro*, the *Dlx5/6*^{-/-} mutant MGE cells showed indistinguishable survival compared to *Dlx5/6*^{+/+} cells for up to 40 days *in vitro* (Supplemental Fig. 7). Furthermore, cell death analysis at embryonic stages (Supplemental Fig. 8) or of the transplanted cortex showed no evidence of increased apoptosis 15 and 30 days after transplantation by TUNEL staining and anti-active caspase-3 immunohistochemistry (data not shown).

Finally, there could be reduced proliferation in the *Dlx5/6*^{-/-} MGE leading to reduced interneuron production. While we have not definitively ruled this out, our analysis of M phase cells (PH3⁺) (Supplemental Fig. 9) and growth in MGE cultures did not detect an obvious phenotype.

Cellular characterization of neocortical interneurons from *Dlx5* BAC transgenic mouse line

The transplantation results show that *Dlx5* and *Dlx5/6* are required for the development of a substantial fraction of PV⁺ neocortical interneurons (Fig. 6). The expression of *Dlx5* and *Dlx6* in maturing and adult cortical interneurons has previously not been examined, thus we sought to explore whether their expression present in PV⁺ interneuron. Unfortunately, we do not have antibodies that specifically detect their DLX5 or DLX6 proteins, and therefore we used other methods to detect their expression. We assessed *Dlx6* expression in the postnatal brain by *in situ* hybridization and by using LacZ expression from the *Dlx6* locus. Neither assay showed robust expression (data not shown), although the Allen Brain Atlas does detect its expression in low numbers of scattered neocortical cells, consistent with its expression in a small subset of interneurons. Thus, in addition to its expression in the

subventricular zone of the MGE and CGE (where it can regulate the early development of cortical interneurons), *Dlx6* may also express in adult cortical interneurons.

To assess *Dlx5* expression, we used the *Dlx5*-GFP BAC transgenic mouse line, in which EGFP reporter gene is inserted immediately upstream of the coding sequence of the *Dlx5* gene. We began by analyzing GFP expression in tangentially migrating cortical interneurons at E15.5. Double-labeling immunohistochemistry was carried out with anti-DLX2 (Kuwajima et al., 2006) and anti-GFP antibodies. We found that not all immature interneurons co-express DLX2 and DLX5 in the marginal zone (MZ), cortical plate (CP) and intermediate zone/subventricular zone (IZ/SVZ) of the developing cortex. Roughly one-third of cells were *Dlx5*-GFP⁻ (Supplemental Fig. 9) (30.18±2.65%, 30.73±2.96% and 41.86±1.96% in MZ, CP and IZ/SVZ, respectively). Furthermore, there was a small subpopulation of *Dlx5*-GFP⁺ cells that were DLX2⁻ (Supplemental Fig.10) (10.21±0.71% in MZ, 10.02±0.67% in CP, 2.25±0.16% in IZ/SVZ, respectively).

Next we examined *Dlx5*-GFP expression in the adult (P60) somatosensory cortex. We assessed its expression among different interneuron populations in layers II-IV and layers V-VI. In layers II-IV, we found that *Dlx5*-GFP was rather evenly distributed among PV⁺, SST⁺, NPY⁺ and CR⁺ interneurons (23.97±2.60% in PV⁺, 17.49±4.95% in SST⁺, 18.11±2.46% in NPY⁺, 30.13±2.4% in CR⁺ interneurons) (Fig.7F). On the other hand in layers V-VI, *Dlx5*-GFP was predominantly expressed in PV⁺ interneurons (45.8 ± 3.75% in PV⁺, 13.75±1.71% in SST⁺, 6.97±1.62% in NPY⁺, 8.62±1.02% in CR⁺ interneurons (Fig. 7G).

We also carried out fate mapping experiments on *Dlx5/6*-lineage neocortical interneurons by crossing *Dlx5/6i-cre* mice (Kohwi et al., 2007) into Rosa-YFP Cre reporter mice. Similarly, we found that GFP⁺ cells were predominately expressed in PV⁺ interneurons in layers V-VI (41.09±1.76% in PV⁺, 15.15±2.35% in SST⁺, 5.37±0.89% in NPY⁺, 8.52±2.05% in CR⁺ interneurons) (Supplemental Fig. 11). Thus, unlike *Dlx1*, which appears to be excluded from PV⁺ interneurons, *Dlx5* is expressed in this interneuron subtype, and, based on our transplantation data, is required for their development.

Spontaneous electrographic seizures and reduced maximum gamma power in *Dlx5/6*^{+/-} heterozygotes in the absence of gross histological abnormalities

Adult *Dlx1*^{-/-} mice exhibit generalized electrographic seizures (Cobos et al. 2005), suggesting that *Dlx5/6* mutants may also have epilepsy. To circumvent the embryonic lethality of *Dlx5/6*^{-/-} mice and determine whether reduced *Dlx5/6* dosage has a functional consequence, we performed video-EEG monitoring and histological studies in adult (4-6 months of age) *Dlx5/6*^{+/-} (heterozygous) mice.

We quantified the total number of cells expressing PV, SST, CR and NPY within a 380,000 μm² region of somatosensory cortex; no significant differences were observed (Fig. 8A-I). Next, we performed video-EEG monitoring on *Dlx5/6*^{+/-} (n = 5) and age-matched littermate control mice (n = 5) greater than 4 months of age during awake, freely moving behavior (Fig. 8J). Seventeen distinct electrographic seizure events (32.5 ± 6.4 sec duration) were confirmed in EEG recordings from four of the five *Dlx5/6*^{+/-} mice. Representative events from *Dlx5/6*^{+/+} and *Dlx5/6*^{+/-} mice are shown in Figure 8J. Electrographic events from *Dlx5/6*^{+/-} mice began with a brief period of high frequency activity evolving into sharp high voltage spikes and polyspike bursting (Fig. 8J-b). Behaviors associated with these events were subtle and sometimes comprised a brief period of arrest with a slight head jerk. Electrographic seizure or behavior was never observed in control animals (Fig. 8J-a). Thus, reduced *Dlx5/6* dosage appears to result in abnormal cortical function (i.e., seizures) despite the absence of gross anatomical abnormalities.

We hypothesized that the cortical hyperexcitability of *Dlx5/6*^{+/-} mice might be due to the functional deficits of PV⁺ interneuron. We based this idea on our evidence that *Dlx5/6* regulate prenatal development of the *Lhx6*⁺ neurons (Fig. 4), and regulate the number and dendritic morphology of PV⁺ cortical interneurons (Fig. 6). Because PV⁺ interneurons are thought to regulate gamma oscillations (Fuchs et al., 2007; Cardin et al., 2009; Sohal et al., 2009), we investigated the power in the different frequency bands in the EEG recording during periods of awake, freely moving mice. First we used wavelet analysis to measure the power in frequency bands between 4 and 200 Hz in EEG recorded from both *Dlx5/6*^{+/+} and *Dlx5/6*^{+/-} mice (n = 4 mice per group). We analyzed five, 60-second long recordings from two sites in each animal. We found that *Dlx5/6*^{+/-} mice exhibited a selective 45 ± 18% increase in the total power between 152-200 Hz (*p* < 0.05 by one-way ANOVA; n = 40 recordings in each group).

Next we investigated whether gamma oscillations were affected in *Dlx5/6*^{+/-} mice. However, because the presence of gamma oscillations is highly dependent on specific behaviors, we reasoned that gamma oscillations might not be present in all of the recordings. Therefore, for each set of recordings (five 60-second recordings from each site in each mouse), we selected the 60-second recording with maximum power in the gamma-range (30-80 Hz). We found that maximum gamma power was reduced by 33 ± 11% in *Dlx5/6*^{+/-} mice (*p* < 0.05 by one-way ANOVA; n = 8 recordings in each group). The reduced maximum gamma power in *Dlx5/6*^{+/-} mice, and the defects in transplanted *Dlx5/6*^{-/-} PV⁺ interneurons, provide evidence that *Dlx5/6* regulate both the development and function of PV⁺ interneurons.

Discussion

We provide evidence that *Dlx5&6* promote the prenatal tangential migration of cortical interneurons, in part through *CXCR4* expression, and that postnatally *Dlx5&6* are preferentially required for the development and dendritic morphology of PV⁺ interneurons. While the cortex of *Dlx5/6*^{+/-} heterozygous mice appears anatomically normal, they have epilepsy and reduced power in their gamma oscillations, suggesting a defect in the function of their PV⁺ interneurons.

Normal patterning and differentiation in the embryonic basal ganglia of the exencephalic *Dlx5/6*^{-/-} mutants

Despite the fact that the embryos are exencephalic (Robledo et al., 2002), we found that regionalization of the telencephalon was remarkably intact, based on the appropriate regional expression of pallial (e.g. *Tbr1*), striatal (e.g. *Ikaros*, *RXRγ*) and pallidal (e.g. *ErbB4*, *Lhx6*) markers, and the generation of subpallium-derived cortical interneurons (Figs. 1, 2, 3, 4, 5; Supplemental Figs. 1, 2). However, because these mutants degenerate after ~E16.5, and because of their exencephalic state, we can't conclude that subpallial differentiation is entirely intact. It is probable that persistent expression of *Dlx1&2* (Fig. 1, 2, 3) can partially compensate for lack of *Dlx5&6*.

Reduced numbers of tangentially migrating *Lhx6*⁺ and *MafB*⁺ cortical interneurons

The cortex of *Dlx5/6*^{-/-} mutants has reduced numbers of cells expressing markers of tangentially migrating immature interneurons (Figs. 2, 3, 4). At E16.5, there is a disproportionate reduction in the expression of *Lhx6* and *MafB* in the MZ, compared to *Dlx1*, suggesting that *Dlx5&6* are preferentially required for the development of some *Lhx6*⁺/*MafB*⁺ cortical interneurons.

There are at least two types of tangentially migrating interneurons: *Dlx*⁺ and *Dlx*⁺;*Lhx6*⁺ (Zhao et al., 2008). *Lhx6* function is required for *MafB* expression and for the production of PV⁺ and SST⁺ interneurons (Liodis et al., 2007; Zhao et al., 2008). Thus, the preferential reduction of *Lhx6* and *MafB* suggests that *Dlx5* & *6* have key roles in the development of PV⁺ and SST⁺ interneurons. Indeed, transplantation of *Dlx5*^{-/-} and *Dlx5/6*^{-/-} mutant MGE cells results in fewer PV⁺ neocortical interneurons (Fig. 6). The observation that SST⁺ interneurons are not reduced supports a hypothesis that *Dlx5* and *Dlx5/6* are more important in promoting the PV subtype; perhaps the subset of *Lhx6*⁺ interneurons that do migrate into the mutant embryonic cortex will become SST⁺.

We have not elucidated the mechanism(s) whereby *Dlx5* and *Dlx5/6* control PV interneuron development. There is clearly a defect in the efficiency of tangential migration and an apparent accumulation of *Lhx6*⁺ cells in the region of the MGE (Fig. 3 arrows). We studied the expression of receptors expressed on the tangentially migrating cells that are implicated in regulating their migration (*CXCR4*, *CXCR7*, *ErbB4*). There was a clear reduction in *CXCR4* expression in cortical SVZ/IZ (Fig. 5). Given *CXCR4*'s known function (Stumm et al., 2003; Li et al., 2008; Liapi et al., 2008; Lopez-Bendito et al., 2008; Tiveron and Cremer, 2008), this defect could contribute to the slowing of tangential migration in the *Dlx5/6*^{-/-} mutants.

Reduced numbers of PV⁺ neocortical interneurons in *Dlx5*^{-/-} and *Dlx5/6*^{-/-} MGE transplants suggests a *Dlx* transcriptional code for interneuron development

Transplantation of mutant MGE into neonatal wild type cortex showed a selective deficit in the formation of PV⁺ interneurons; there was a ~2-fold reduction in *Dlx5*^{-/-} transplants and a ~3 fold reduction in the *Dlx5/6*^{-/-} transplants (Fig. 6). It strongly suggests a cell-autonomous requirement for *Dlx5/6* in the development of PV⁺ interneurons. The *Dlx5*^{-/-} phenotype was less severe than *Dlx5/6*^{-/-} phenotype; this provides evidence that *Dlx6* contributes to the development of PV⁺ interneurons. *Dlx6* expression is weakly detected in the MGE SVZ (Anderson et al., 1997b), where it could, in conjunction with *Dlx5*, promote *Lhx6* expression. Notably, *Dlx1/2*^{-/-} mutants have a modest reduction in *Lhx6* expression in the MGE SVZ (Petryniak et al., 2007). However, there is no obvious reduction in *Lhx6* (or *Lhx6*-GFP) expression in the *Dlx5/6*^{-/-} MGE SVZ; rather there may be increased expression (Figs. 2 and 3). It is possible that *Dlx5/6* promote *Lhx6* expression in developing PV⁺ interneurons, and not in developing SST⁺ interneurons. Alternatively, lack of *Dlx5/6* could alter cell identity. While there is no definitive data showing this, there is a slight increase in SST⁺ cells in the transplants (Fig. 6).

PV⁺ and SST⁺ interneurons appear to arise preferentially from distinct dorsoventral domains of the MGE (Flames et al., 2007). The genetic mechanisms that differentially regulate their development are just beginning to be understood. Prenatally, *Dlx1* and *Lhx6* are initially expressed in most migrating interneurons; late in gestation a larger subset express only *Dlx1* (Zhao et al., 2008). By adulthood, their expression becomes further restricted to specific subtypes. *Dlx1* expression is not detected in PV⁺ interneurons, whereas it is expressed in most CR⁺ interneurons and subsets of SST⁺ and NPY⁺ interneurons; *Lhx6* is expressed in most PV⁺ and SST⁺ interneurons and a small subsets of CR⁺ and NPY⁺ interneurons (Cobos et al., 2005). Here we show that while *Dlx5* is broadly expressed prenatally in migrating interneurons, its expression in adult deep cortical layers is preferentially restricted to PV⁺ interneurons (Fig. 7A-H). Thus, current evidence supports a model that *Dlx1* and *Dlx5* show differential expression and function in distinct subtypes of cortical interneurons: *Dlx1* in *Lhx6*⁻ interneurons that express SST, CR and NPY, and *Dlx5* in *Lhx6*⁺ interneurons that express PV (Fig. 7H).

Spontaneous electrographic seizures and reduced maximum gamma power in *Dlx5/6*^{+/-} heterozygotes

Clinical and experimental evidence demonstrating an impairment of GABA-mediated inhibition in epilepsy is quite common (Treiman, 2001). Loss of GABA-producing interneurons is considered a critical aspect of this impairment and has been observed in tissue sections from patients with intractable epilepsy (Knopp et al., 2008) and, more recently, in mutant mice (Powell et al., 2003; Cobos et al., 2005; Marsh et al., 2005; Glickstein et al., 2007; Butt et al., 2008; Marsh et al., 2009). These findings contribute to an emerging concept that epileptic disorders associated with interneuron dysfunction could be classified as an “interneuronopathy” (Kato and Dobyns, 2005). Our analysis of *Dlx5/6*^{+/-} mutants is consistent with this classification and indicates that reduced *Dlx5/6* dosage results in brief spontaneous electrographic seizures. This is an interesting finding given that we did not detect a frank decrease in interneuron density in the cortex or hippocampus of these animals. However, because we did observe impairment in the dendritic/axonal arbors of PV⁺ interneurons from *Dlx5/6*^{-/-} mutant transplants, these findings suggest that epilepsy can be associated with subtle changes in interneuron structure. That altered PV⁺ interneuron morphology leads to functional impairment was further confirmed in our observations of reduced gamma power in the EEG recordings; gamma waves a signature of PV⁺ interneuron function (Fuchs et al., 2007; Cardin et al., 2009; Sohal et al., 2009). As such, we hypothesize that *Dlx5/6* regulates postnatal properties of PV⁺ interneurons. Future studies are needed to establish the cellular and molecular basis of this physiological phenotype, although clues could be found in the recent paper describing developmental gene expression in PV⁺ interneurons (Okaty et al., 2009).

The observation of electrophysiological defects in *Dlx5/6*^{+/-} mice is important as it provides the first evidence that reduced gene dosage (heterozygosity of a loss of function allele) of transcription factors result in epilepsy, and yet show no obvious anatomical defect (Fig. 8). This finding may be germane to human neuropsychiatric disorders, where geneticists are discovering mutations in heterozygosity states. For instance, we have identified autistic probands who are heterozygous for two types of non-synonymous mutations in *Dlx5* (Hamilton et al., 2005).

Supplementary Material

Refer to Web version on PubMed Central for supplementary material.

Acknowledgments

This work was supported by the research grants to: JLRR from Nina Ireland, the Larry L. Hillblom Foundation, NIMH R01 and R37 MH49428-01, and K05 MH065670; to YW from C.U.R.E Rhode Island Award from the Epilepsy Foundation; to CAD from NARSAD; to VSS from a T32 postdoctoral training fellowship from NIMH; to KD from Stanford, BioX/Bioengineering, NIMH, NIDA, NSF, CIRM, HHMI, and the McKnight, Coulter, Kinetics, and Keck Foundations; and to SCB from NIH grant 5R01NS048528.

References

- Anderson SA, Eisenstat DD, Shi L, Rubenstein JL. Interneuron migration from basal forebrain to neocortex: dependence on *Dlx* genes. *Science* 1997a;278:474–476. [PubMed: 9334308]
- Anderson SA, Qiu M, Bulfone A, Eisenstat DD, Meneses J, Pedersen R, Rubenstein JL. Mutations of the homeobox genes *Dlx-1* and *Dlx-2* disrupt the striatal subventricular zone and differentiation of late born striatal neurons. *Neuron* 1997b;19:27–37. [PubMed: 9247261]
- Baraban SC, Southwell DG, Estrada RC, Jones DL, Sebe JY, Alfaro-Cervello C, Garcia-Verdugo JM, Rubenstein JL, Alvarez-Buylla A. Reduction of seizures by transplantation of cortical GABAergic

- interneuron precursors into Kv1.1 mutant mice. *Proc Natl Acad Sci U S A* 2009;106:15472–15477. [PubMed: 19706400]
- Bielle F, Griveau A, Narboux-Neme N, Vigneau S, Sigrist M, Arber S, Wassef M, Pierani A. Multiple origins of Cajal-Retzius cells at the borders of the developing pallium. *Nat Neurosci* 2005;8:1002–1012. [PubMed: 16041369]
- Borrell V, Marin O. Meninges control tangential migration of hem-derived Cajal-Retzius cells via CXCL12/CXCR4 signaling. *Nat Neurosci* 2006;9:1284–1293. [PubMed: 16964252]
- Butt SJ, Fuccillo M, Nery S, Noctor S, Kriegstein A, Corbin JG, Fishell G. The temporal and spatial origins of cortical interneurons predict their physiological subtype. *Neuron* 2005;48:591–604. [PubMed: 16301176]
- Butt SJ, Sousa VH, Fuccillo MV, Hjerling-Leffler J, Miyoshi G, Kimura S, Fishell G. The requirement of Nkx2-1 in the temporal specification of cortical interneuron subtypes. *Neuron* 2008;59:722–732. [PubMed: 18786356]
- Cardin JA, Carlen M, Meletis K, Knoblich U, Zhang F, Deisseroth K, Tsai LH, Moore CI. Driving fast-spiking cells induces gamma rhythm and controls sensory responses. *Nature* 2009;459:663–667. [PubMed: 19396156]
- Cobos I, Borello U, Rubenstein JL. Dlx transcription factors promote migration through repression of axon and dendrite growth. *Neuron* 2007;54:873–888. [PubMed: 17582329]
- Cobos I, Long JE, Thwin MT, Rubenstein JL. Cellular patterns of transcription factor expression in developing cortical interneurons. *Cereb Cortex* 2006;16 1:i82–88. [PubMed: 16766712]
- Cobos I, Calcagnotto ME, Vilaythong AJ, Thwin MT, Noebels JL, Baraban SC, Rubenstein JL. Mice lacking Dlx1 show subtype-specific loss of interneurons, reduced inhibition and epilepsy. *Nat Neurosci* 2005;8:1059–1068. [PubMed: 16007083]
- Colasante G, Collombat P, Raimondi V, Bonanomi D, Ferrai C, Maira M, Yoshikawa K, Mansouri A, Valtorta F, Rubenstein JL, Broccoli V. Arx is a direct target of Dlx2 and thereby contributes to the tangential migration of GABAergic interneurons. *J Neurosci* 2008;28:10674–10686. [PubMed: 18923043]
- Colombo E, Collombat P, Colasante G, Bianchi M, Long J, Mansouri A, Rubenstein JL, Broccoli V. Inactivation of Arx, the murine ortholog of the X-linked lissencephaly with ambiguous genitalia gene, leads to severe disorganization of the ventral telencephalon with impaired neuronal migration and differentiation. *J Neurosci* 2007;27:4786–4798. [PubMed: 17460091]
- Depew MJ, Lufkin T, Rubenstein JL. Specification of jaw subdivisions by Dlx genes. *Science* 2002;298:381–385. [PubMed: 12193642]
- Du T, Xu Q, Ocbina PJ, Anderson SA. NKX2.1 specifies cortical interneuron fate by activating Lhx6. *Development* 2008;135:1559–1567. [PubMed: 18339674]
- Flames N, Marin O. Developmental mechanisms underlying the generation of cortical interneuron diversity. *Neuron* 2005;46:377–381. [PubMed: 15882635]
- Flames N, Pla R, Gelman DM, Rubenstein JL, Puelles L, Marin O. Delineation of multiple subpallial progenitor domains by the combinatorial expression of transcriptional codes. *J Neurosci* 2007;27:9682–9695. [PubMed: 17804629]
- Fogarty M, Grist M, Gelman D, Marin O, Pachnis V, Kessaris N. Spatial genetic patterning of the embryonic neuroepithelium generates GABAergic interneuron diversity in the adult cortex. *J Neurosci* 2007;27:10935–10946. [PubMed: 17928435]
- Fuchs EC, Zivkovic AR, Cunningham MO, Middleton S, Lebeau FE, Bannerman DM, Rozov A, Whittington MA, Traub RD, Rawlins JN, Monyer H. Recruitment of parvalbumin-positive interneurons determines hippocampal function and associated behavior. *Neuron* 2007;53:591–604. [PubMed: 17296559]
- Fulp CT, Cho G, Marsh ED, Nasrallah IM, Labosky PA, Golden JA. Identification of Arx transcriptional targets in the developing basal forebrain. *Hum Mol Genet* 2008;17:3740–3760. [PubMed: 18799476]
- Glickstein SB, Moore H, Slowinska B, Racchumi J, Suh M, Chuhma N, Ross ME. Selective cortical interneuron and GABA deficits in cyclin D2-null mice. *Development* 2007;134:4083–4093. [PubMed: 17965053]

- Hamilton SP, Woo JM, Carlson EJ, Ghanem N, Ekker M, Rubenstein JL. Analysis of four DLX homeobox genes in autistic probands. *BMC Genet* 2005;6:52. [PubMed: 16266434]
- Hammond V, So E, Gunnarsen J, Valcanis H, Kalloniatis M, Tan SS. Layer positioning of late-born cortical interneurons is dependent on Reelin but not p35 signaling. *J Neurosci* 2006;26:1646–1655. [PubMed: 16452688]
- Hevner RF, Daza RA, Englund C, Kohtz J, Fink A. Postnatal shifts of interneuron position in the neocortex of normal and reeler mice: evidence for inward radial migration. *Neuroscience* 2004;124:605–618. [PubMed: 14980731]
- Kato M, Dobyns WB. X-linked lissencephaly with abnormal genitalia as a tangential migration disorder causing intractable epilepsy: proposal for a new term, “interneuronopathy”. *J Child Neurol* 2005;20:392–397. [PubMed: 15921244]
- Kitamura K, Yanazawa M, Sugiyama N, Miura H, Iizuka-Kogo A, Kusaka M, Omichi K, Suzuki R, Kato-Fukui Y, Kamiirisa K, Matsuo M, Kamijo S, Kasahara M, Yoshioka H, Ogata T, Fukuda T, Kondo I, Kato M, Dobyns WB, Yokoyama M, Morohashi K. Mutation of ARX causes abnormal development of forebrain and testes in mice and X-linked lissencephaly with abnormal genitalia in humans. *Nat Genet* 2002;32:359–369. [PubMed: 12379852]
- Knopp A, Frahm C, Fidzinski P, Witte OW, Behr J. Loss of GABAergic neurons in the subiculum and its functional implications in temporal lobe epilepsy. *Brain* 2008;131:1516–1527. [PubMed: 18504292]
- Kohwi M, Petryniak MA, Long JE, Ekker M, Obata K, Yanagawa Y, Rubenstein JL, Alvarez-Buylla A. A subpopulation of olfactory bulb GABAergic interneurons is derived from Emx1- and Dlx5/6-expressing progenitors. *J Neurosci* 2007;27:6878–6891. [PubMed: 17596436]
- Kuwajima T, Nishimura I, Yoshikawa K. Necdin promotes GABAergic neuron differentiation in cooperation with Dlx homeodomain proteins. *J Neurosci* 2006;26:5383–5392. [PubMed: 16707790]
- Levi G, Puche AC, Mantero S, Barbieri O, Trombino S, Paleari L, Egeo A, Merlo GR. The Dlx5 homeodomain gene is essential for olfactory development and connectivity in the mouse. *Mol Cell Neurosci* 2003;22:530–543. [PubMed: 12727448]
- Li G, Adesnik H, Li J, Long J, Nicoll RA, Rubenstein JL, Pleasure SJ. Regional distribution of cortical interneurons and development of inhibitory tone are regulated by Cxcl12/Cxcr4 signaling. *J Neurosci* 2008;28:1085–1098. [PubMed: 18234887]
- Liapi A, Pritchett J, Jones O, Fujii N, Parnavelas JG, Nadarajah B. Stromal-derived factor 1 signalling regulates radial and tangential migration in the developing cerebral cortex. *Dev Neurosci* 2008;30:117–131. [PubMed: 18075260]
- Liodis P, Denaxa M, Grigoriou M, Akufo-Addo C, Yanagawa Y, Pachnis V. Lhx6 activity is required for the normal migration and specification of cortical interneuron subtypes. *J Neurosci* 2007;27:3078–3089. [PubMed: 17376969]
- Long JE, Cobos I, Potter GB, Rubenstein JL. Dlx1 and Mash1 Transcription Factors Control MGE and CGE Patterning and Differentiation through Parallel and Overlapping Pathways. *Cereb Cortex* 2009a;19:i96–i106. [PubMed: 19386638]
- Long JE, Garel S, Depew MJ, Tobet S, Rubenstein JL. DLX5 regulates development of peripheral and central components of the olfactory system. *J Neurosci* 2003;23:568–578. [PubMed: 12533617]
- Long JE, Swan C, Liang WS, Cobos I, Potter GB, Rubenstein JL. Dlx1&2 and Mash1 transcription factors control striatal patterning and differentiation through parallel and overlapping pathways. *J Comp Neurol* 2009b;512:556–572. [PubMed: 19030180]
- Long JE, Garel S, Alvarez-Dolado M, Yoshikawa K, Osumi N, Alvarez-Buylla A, Rubenstein JL. Dlx-dependent and -independent regulation of olfactory bulb interneuron differentiation. *J Neurosci* 2007;27:3230–3243. [PubMed: 17376983]
- Lopez-Bendito G, Sanchez-Alcaniz JA, Pla R, Borrell V, Pico E, Valdeolmillos M, Marin O. Chemokine signaling controls intracortical migration and final distribution of GABAergic interneurons. *J Neurosci* 2008;28:1613–1624. [PubMed: 18272682]
- Marin O, Anderson SA, Rubenstein JL. Origin and molecular specification of striatal interneurons. *J Neurosci* 2000;20:6063–6076. [PubMed: 10934256]

- Marin O, Plump AS, Flames N, Sanchez-Camacho C, Tessier-Lavigne M, Rubenstein JL. Directional guidance of interneuron migration to the cerebral cortex relies on subcortical Slit1/2-independent repulsion and cortical attraction. *Development* 2003;130:1889–1901. [PubMed: 12642493]
- Marsh E, Melamed SE, Barron T, Clancy RR. Migrating partial seizures in infancy: expanding the phenotype of a rare seizure syndrome. *Epilepsia* 2005;46:568–572. [PubMed: 15816952]
- Marsh E, Fulp C, Gomez E, Nasrallah I, Minarcik J, Sudi J, Christian SL, Mancini G, Labosky P, Dobyns W, Brooks-Kayal A, Golden JA. Targeted loss of Arx results in a developmental epilepsy mouse model and recapitulates the human phenotype in heterozygous females. *Brain* 2009;132:1563–1576. [PubMed: 19439424]
- Okaty BW, Miller MN, Sugino K, Hempel CM, Nelson SB. Transcriptional and electrophysiological maturation of neocortical fast-spiking GABAergic interneurons. *J Neurosci* 2009;29:7040–7052. [PubMed: 19474331]
- Petryniak MA, Potter GB, Rowitch DH, Rubenstein JL. Dlx1 and Dlx2 control neuronal versus oligodendroglial cell fate acquisition in the developing forebrain. *Neuron* 2007;55:417–433. [PubMed: 17678855]
- Pla R, Borrell V, Flames N, Marin O. Layer acquisition by cortical GABAergic interneurons is independent of Reelin signaling. *J Neurosci* 2006;26:6924–6934. [PubMed: 16807322]
- Pleasure SJ, Anderson S, Hevner R, Bagri A, Marin O, Lowenstein DH, Rubenstein JL. Cell migration from the ganglionic eminences is required for the development of hippocampal GABAergic interneurons. *Neuron* 2000;28:727–740. [PubMed: 11163262]
- Powell EM, Campbell DB, Stanwood GD, Davis C, Noebels JL, Levitt P. Genetic disruption of cortical interneuron development causes region- and GABA cell type-specific deficits, epilepsy, and behavioral dysfunction. *J Neurosci* 2003;23:622–631. [PubMed: 12533622]
- Robledo RF, Rajan L, Li X, Lufkin T. The Dlx5 and Dlx6 homeobox genes are essential for craniofacial, axial, and appendicular skeletal development. *Genes Dev* 2002;16:1089–1101. [PubMed: 12000792]
- Sohal VS, Zhang F, Yizhar O, Deisseroth K. Parvalbumin neurons and gamma rhythms enhance cortical circuit performance. *Nature* 2009;459:698–702. [PubMed: 19396159]
- Stumm RK, Zhou C, Ara T, Lazarini F, Dubois-Dalcq M, Nagasawa T, Holtt V, Schulz S. CXCR4 regulates interneuron migration in the developing neocortex. *J Neurosci* 2003;23:5123–5130. [PubMed: 12832536]
- Sussel L, Marin O, Kimura S, Rubenstein JL. Loss of Nkx2.1 homeobox gene function results in a ventral to dorsal molecular respecification within the basal telencephalon: evidence for a transformation of the pallidum into the striatum. *Development* 1999;126:3359–3370. [PubMed: 10393115]
- Tiveron MC, Cremer H. CXCL12/CXCR4 signalling in neuronal cell migration. *Curr Opin Neurobiol* 2008
- Treiman DM. GABAergic mechanisms in epilepsy. *Epilepsia* 2001;42 3:8–12. [PubMed: 11520315]
- Wonders CP, Anderson SA. The origin and specification of cortical interneurons. *Nat Rev Neurosci* 2006;7:687–696. [PubMed: 16883309]
- Xu Q, Tam M, Anderson SA. Fate mapping Nkx2.1-lineage cells in the mouse telencephalon. *J Comp Neurol* 2008;506:16–29. [PubMed: 17990269]
- Xu Q, Cobos I, De La Cruz E, Rubenstein JL, Anderson SA. Origins of cortical interneuron subtypes. *J Neurosci* 2004;24:2612–2622. [PubMed: 15028753]
- Yabut O, Renfro A, Niu S, Swann JW, Marin O, D'Arcangelo G. Abnormal laminar position and dendrite development of interneurons in the reeler forebrain. *Brain Res* 2007;1140:75–83. [PubMed: 16996039]
- Yun K, Fischman S, Johnson J, Hrabe de Angelis M, Weinmaster G, Rubenstein JL. Modulation of the notch signaling by Mash1 and Dlx1/2 regulates sequential specification and differentiation of progenitor cell types in the subcortical telencephalon. *Development* 2002;129:5029–5040. [PubMed: 12397111]
- Zerucha T, Stuhmer T, Hatch G, Park BK, Long Q, Yu G, Gambarotta A, Schultz JR, Rubenstein JL, Ekker M. A highly conserved enhancer in the Dlx5/Dlx6 intergenic region is the site of cross-

regulatory interactions between Dlx genes in the embryonic forebrain. *J Neurosci* 2000;20:709–721. [PubMed: 10632600]

Zhao Y, Flandin P, Long JE, Cuesta MD, Westphal H, Rubenstein JL. Distinct molecular pathways for development of telencephalic interneuron subtypes revealed through analysis of Lhx6 mutants. *J Comp Neurol* 2008;510:79–99. [PubMed: 18613121]

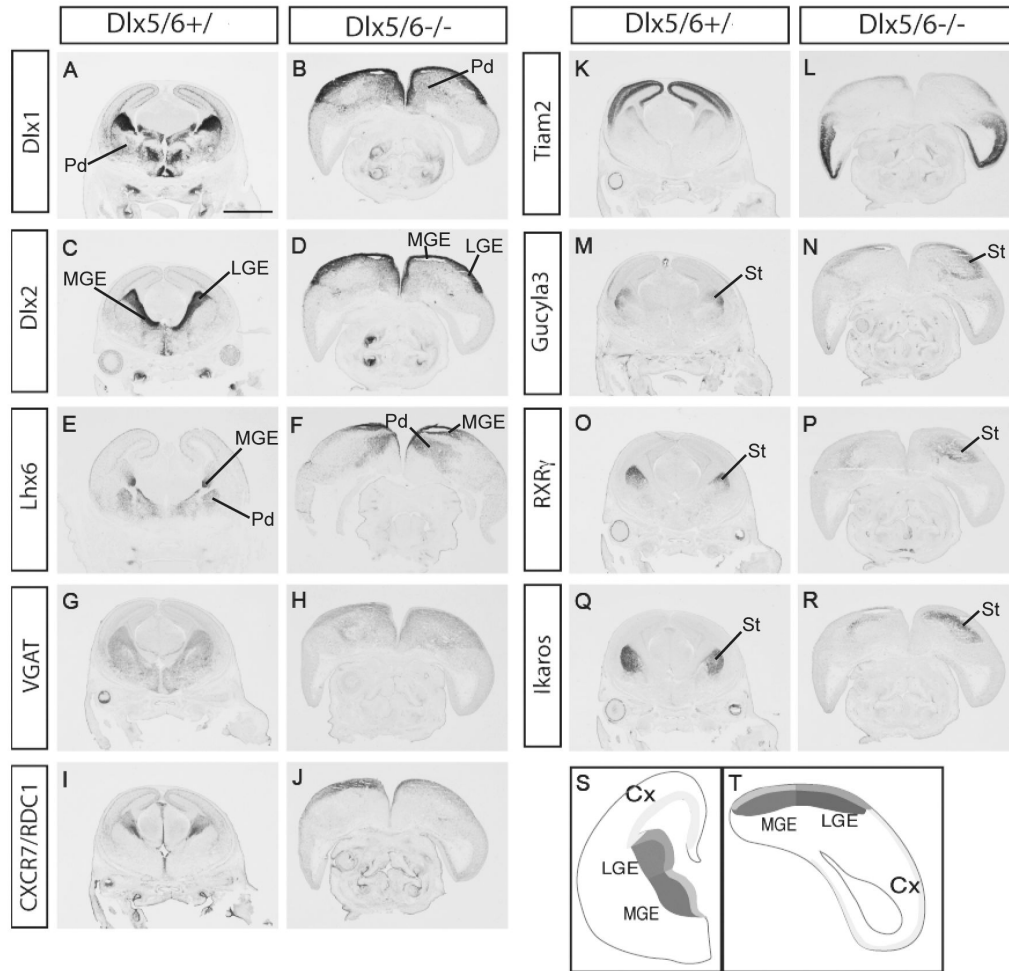


Figure 1.

Preservation of telencephalic regional patterning, and features of subpallial differentiation, in E15.5 *Dlx5/6*^{-/-} mutants. The *Dlx5/6*^{-/-} mutants are exencephalic; a schematic representation of *Dlx5/6*^{+/+} (S) and *Dlx5/6*^{-/-} (T) is presented to help orient the reader to the regions of the exencephalic telencephalon. Coronal sections from *Dlx5/6*^{+/+} and *Dlx5/6*^{-/-} were labeled by *in situ* hybridization with markers of LGE and MGE progenitor and mantle zones; the *Dlx5/6*^{-/-} mutants do not show major gene expression defects, although the morphologies of the telencephalic regions are abnormal (A~R). Abbreviations: cx: cortex; lge: lateral ganglionic eminence; mge: medial ganglionic eminence; pd: pallidum (including globus pallidus); st: striatum. Scale bar: 1.5mm.

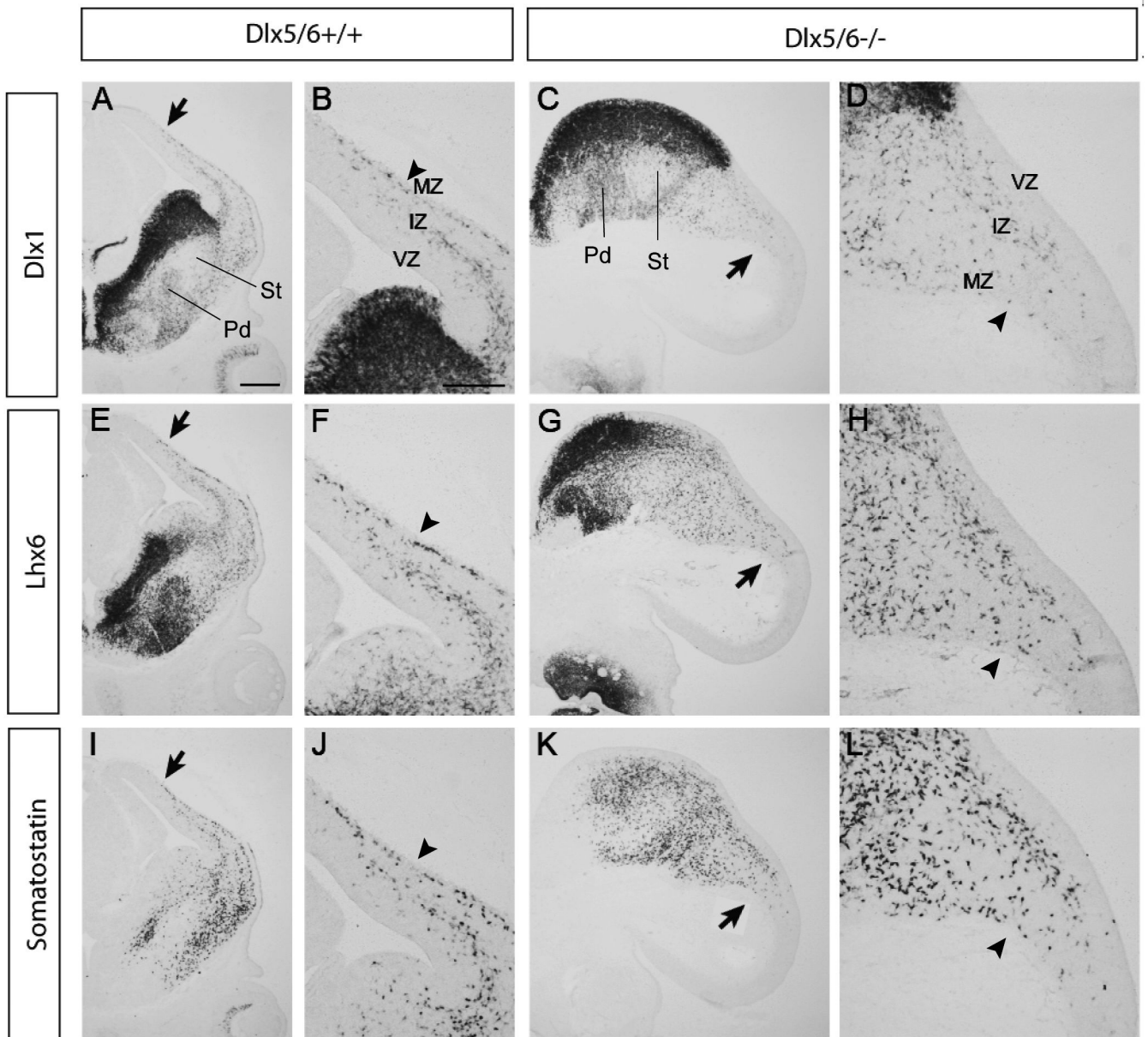


Figure 2. Reduced tangential migration in *Dlx5/6*^{-/-} mutants at E13.5. Coronal sections from *Dlx5/6*^{+/+} and *Dlx5/6*^{-/-} were labeled by *in situ* hybridization against *Dlx1* (A~D), *Lhx6* (E~H) and *Somatostatin* (I~L). The arrows point to the leading migrating cells. Note superficial migratory stream (arrowheads) in MZ is poorly formed in *Dlx5/6*^{-/-} mutants. Abbreviations: IZ: intermediate zone; MZ: marginal zone; VZ: ventricular zone. Scale bars: A, E, I, C, G, K, 300 μ m; B, D, F, H, J, L, 200 μ m.

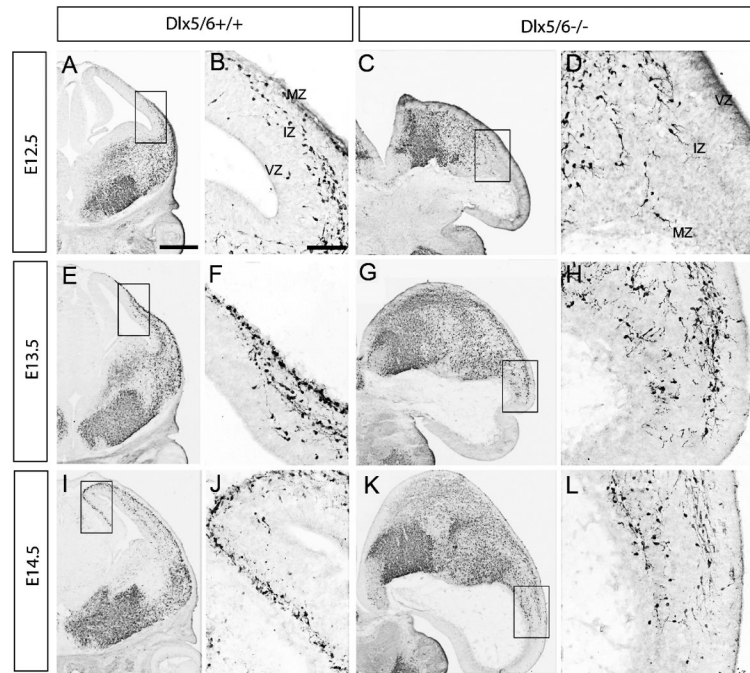


Figure 3. Reduced tangential migration and accumulation of Lhx6-GFP positive cells in the SVZ of the LGE of *Dlx5/6*^{-/-} mutants at E12.5, E13.5 and E14.5. Immunohistochemistry for GFP was carried out on coronal sections from E12.5 (A~D), E13.5 (E~H) and E14.5 (I~L) *Dlx5/6*^{+/+} and *Dlx5/6*^{-/-} mutants. Boxed areas shown in high magnification are the migrating cells at the front of migration. *Dlx5/6*^{-/-} mutants show reduced tangential migration and an accumulation of Lhx6-GFP cells in the SVZ of the LGE. Abbreviations: IZ: intermediate zone; MZ: marginal zone; VZ: ventricular zone. Scale bars: A, C, E, G, I, K, 500µm; B, D, F, H, J, L, 200µm.

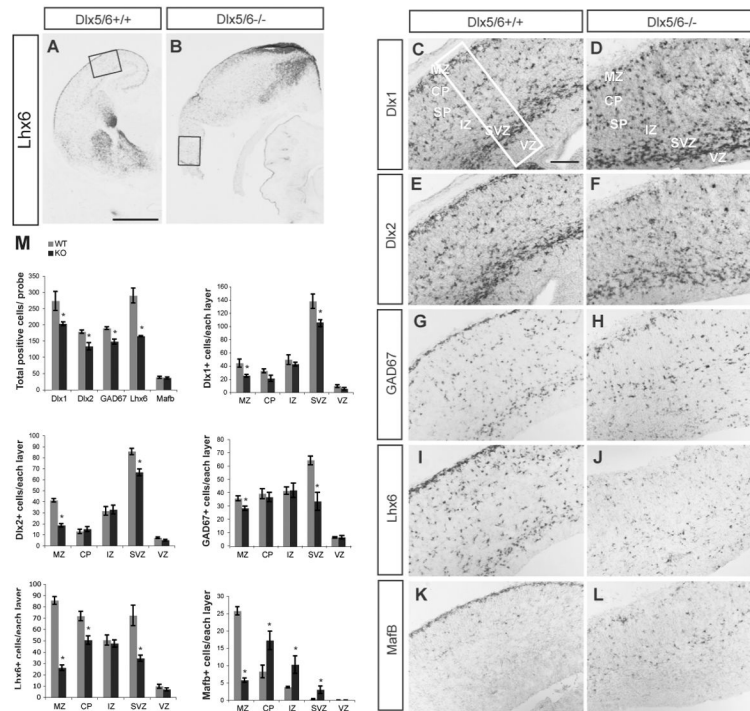


Figure 4.

Reduced number of *Dlx1*⁺, *Dlx2*⁺, *GAD67*⁺, *Lhx6*⁺ cells in the lateral cortex of *Dlx5/6*^{-/-} mutants at E16.5. *in situ* hybridization with probes for *Lhx6* (A, B, I, J), *Dlx1* (C,D), *Dlx2* (E, F), *GAD67* (G, H), and *MafB* (K,L) was carried out on coronal sections of *Dlx5/6*^{+/+} and *Dlx5/6*^{-/-} mutants. The boxes in A and B show the region that is shown at higher magnification in C-L. The box in C shows the size of the region used for cell counting; the total number of cells expressing these genes within 125,000 μm^2 of the lateral neocortex and the number of positive cells in each of the cortical layers are presented (M). The reduction is most severe in MZ and SVZ, particularly for *Lhx6* and *MafB* within the MZ. Abbreviations: CP: cortical plate; IZ: intermediate zone; MZ: marginal zone; SVZ: subventricular zone; VZ: ventricular zone. Scale bars: A, B, 1mm; C~L, 200 μm .

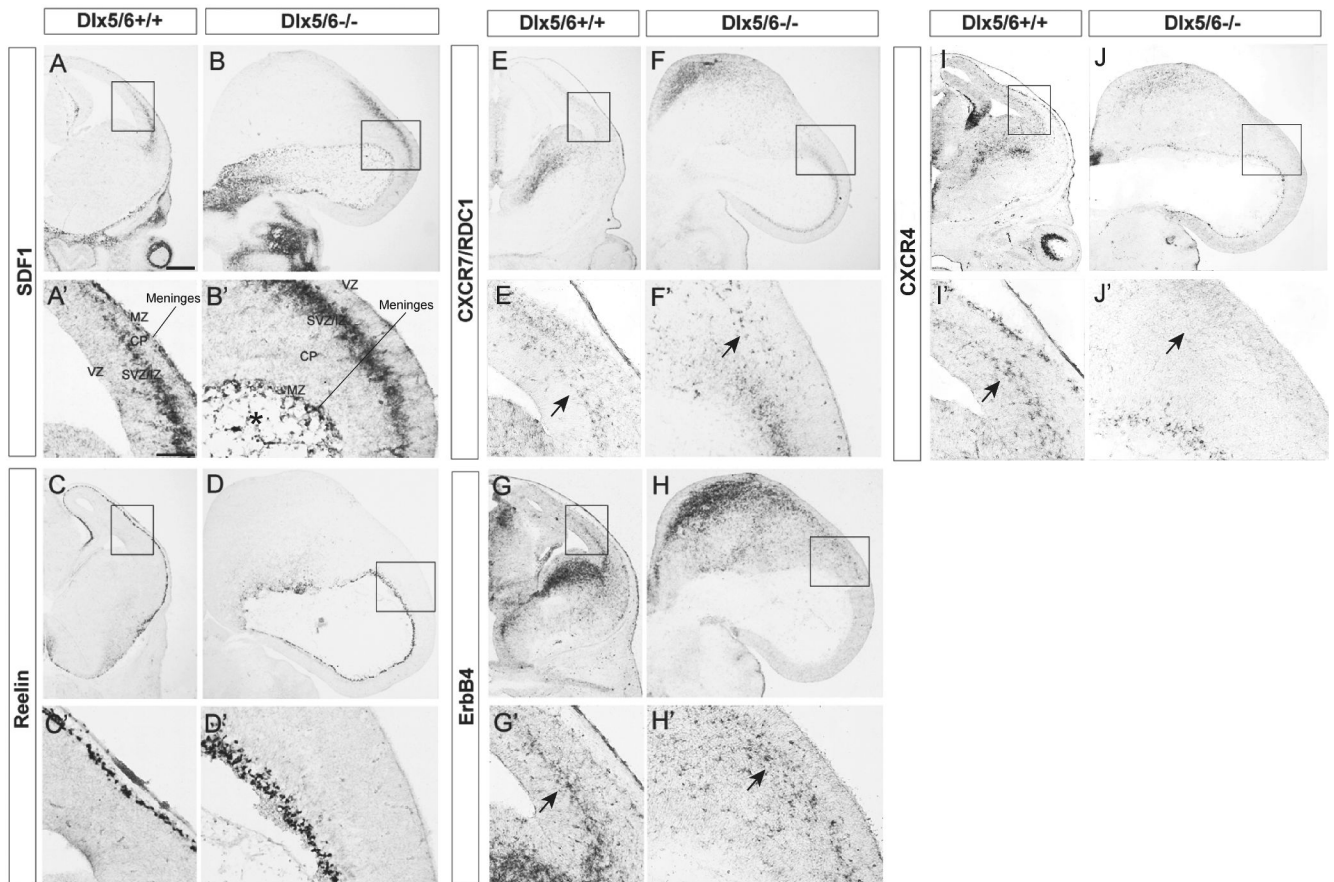
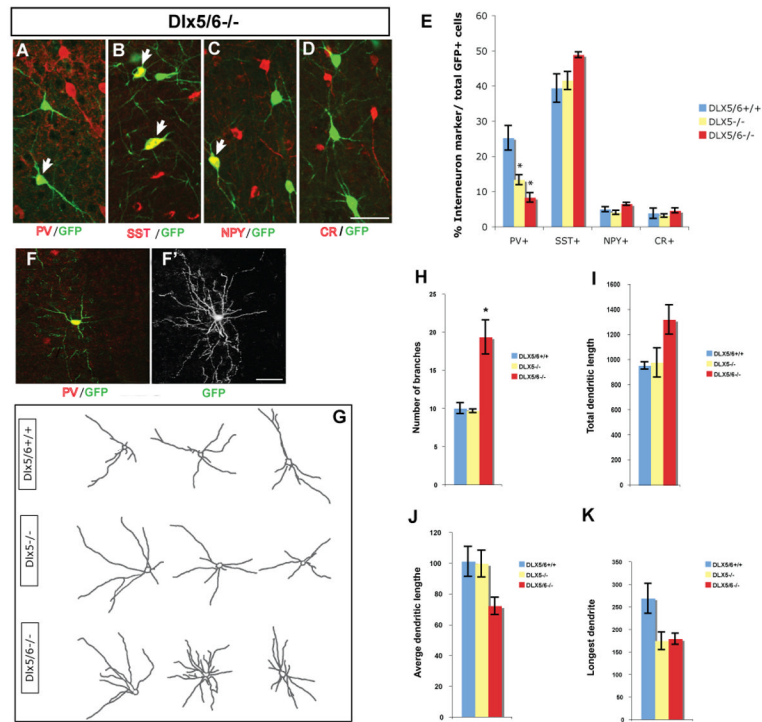


Figure 5.

Loss *CXCR4* expression in deep migratory interneurons of *Dlx5/6*^{-/-} mutants at E13.5. Coronal sections from *Dlx5/6*^{+/+} (A, C, E, G, I) and *Dlx5/6*^{-/-} (B, D, F, H, J) were labeled by in situ hybridization against *SDF1*, *Reelin*, *CXCR7* (*RDC1*), *ErbB4* and *CXCR4*. Boxed areas are shown below in high magnification. The expression *SDF1* and *reelin* was maintained in *Dlx5/6*^{-/-} mutants (B,D). The cavity formed by the everted exencephalic cortex contained scattered *SDF1*⁺ cells. (* in B') Although the expression of *CXCR7* and *ErbB4* was intact, *CXCR4* expression was not detected in deep migratory interneurons (arrows in E', F', G', H', I', J'). Abbreviations: CP: cortical plate; IZ: intermediate zone; MZ: marginal zone; SVZ: subventricular zone; VZ: ventricular zone. Scale bar: 300μm.

**Figure 6.**

Cell-autonomous role for *Dlx5/6* in controlling differentiation of PV⁺ cortical interneurons. E13.5 *Dlx5*^{-/-} or *Dlx5/6*^{-/-} mutant MGE cells were transplanted into a wild type postnatal day 0 (P0) cortex; the Lhx6-BAC GFP transgene was a reporter to follow the fate of MGE-derived cells several weeks after transplantation. (A~D) Neocortical interneurons differentiated from transplanted Lhx6-GFP-expressing *Dlx5/6*^{-/-} precursors, as shown by double immunofluorescence with anti-PV, anti-SST, anti-NPY or anti-CR antibodies. E. Percentage of double-labeled cells in the neocortex of 2-month-old mice grafted with control (blue), *Dlx5*^{-/-} (yellow) and *Dlx5/6*^{-/-} (red) cells. The percentage of GFP⁺/PV⁺ double-positive cells is reduced in mice grafted with either the *Dlx5*^{-/-} or *Dlx5/6*^{-/-} MGE cells. To analyze the morphology of GFP⁺/PV⁺ interneurons, Z-stack confocal image for dendrite analysis was used; a representative GFP⁺/PV⁺ grafted cell from *Dlx5/6*^{-/-} mutant is shown (F); the same cell was captured with Z-stack confocal image for dendrite analysis (F'). (G) Representative images of grafted PV⁺ neocortical interneurons from control, *Dlx5*^{-/-} and *Dlx5/6*^{-/-} mutants. (H~K) Quantification of dendrite branching of PV⁺ interneurons from control (blue), *Dlx5*^{-/-} (yellow) and *Dlx5/6*^{-/-} (red) mutants. Note that, the number of branches is increased in *Dlx5/6*^{-/-} grafted PV⁺ interneurons. Scale bar: 100µm.

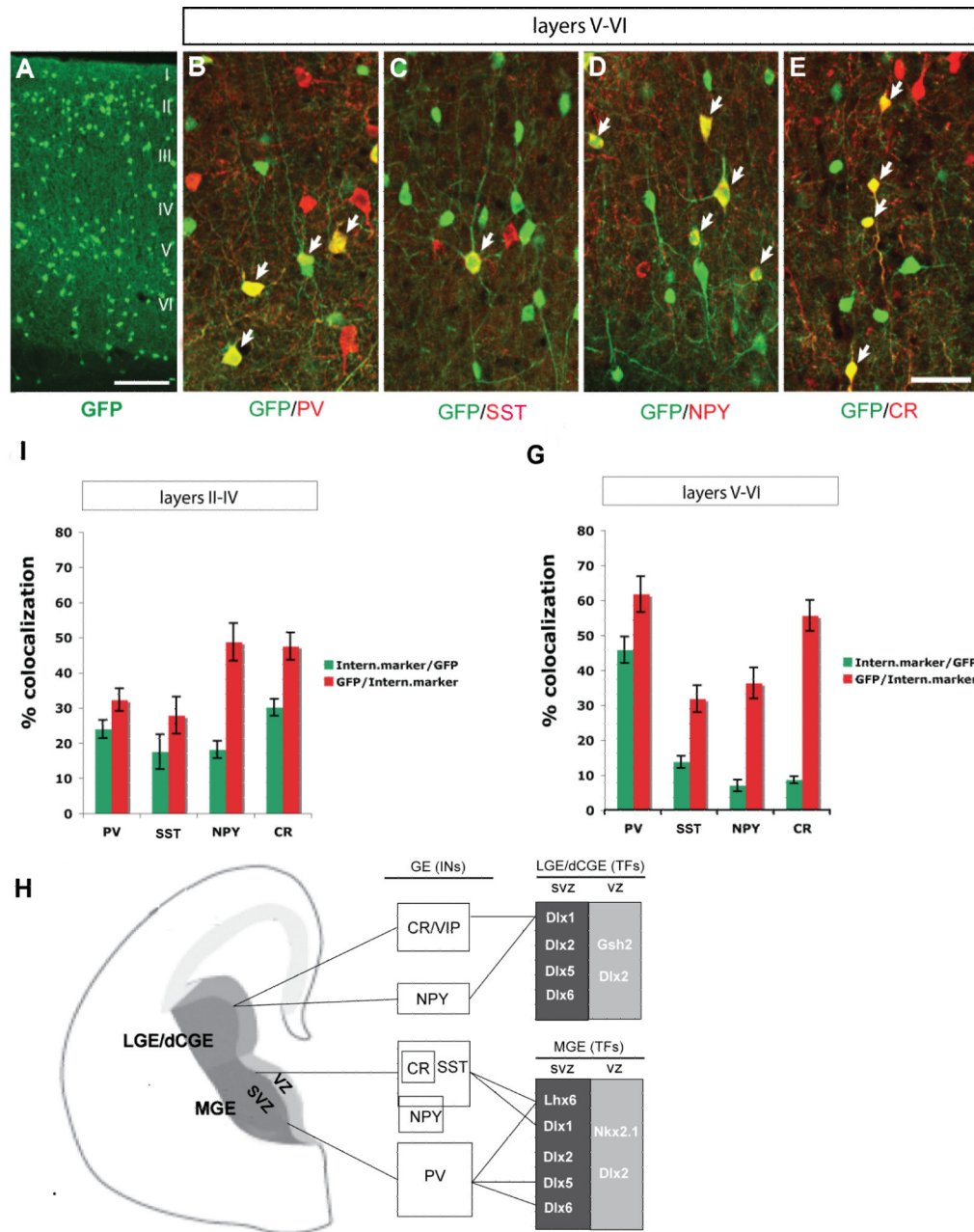
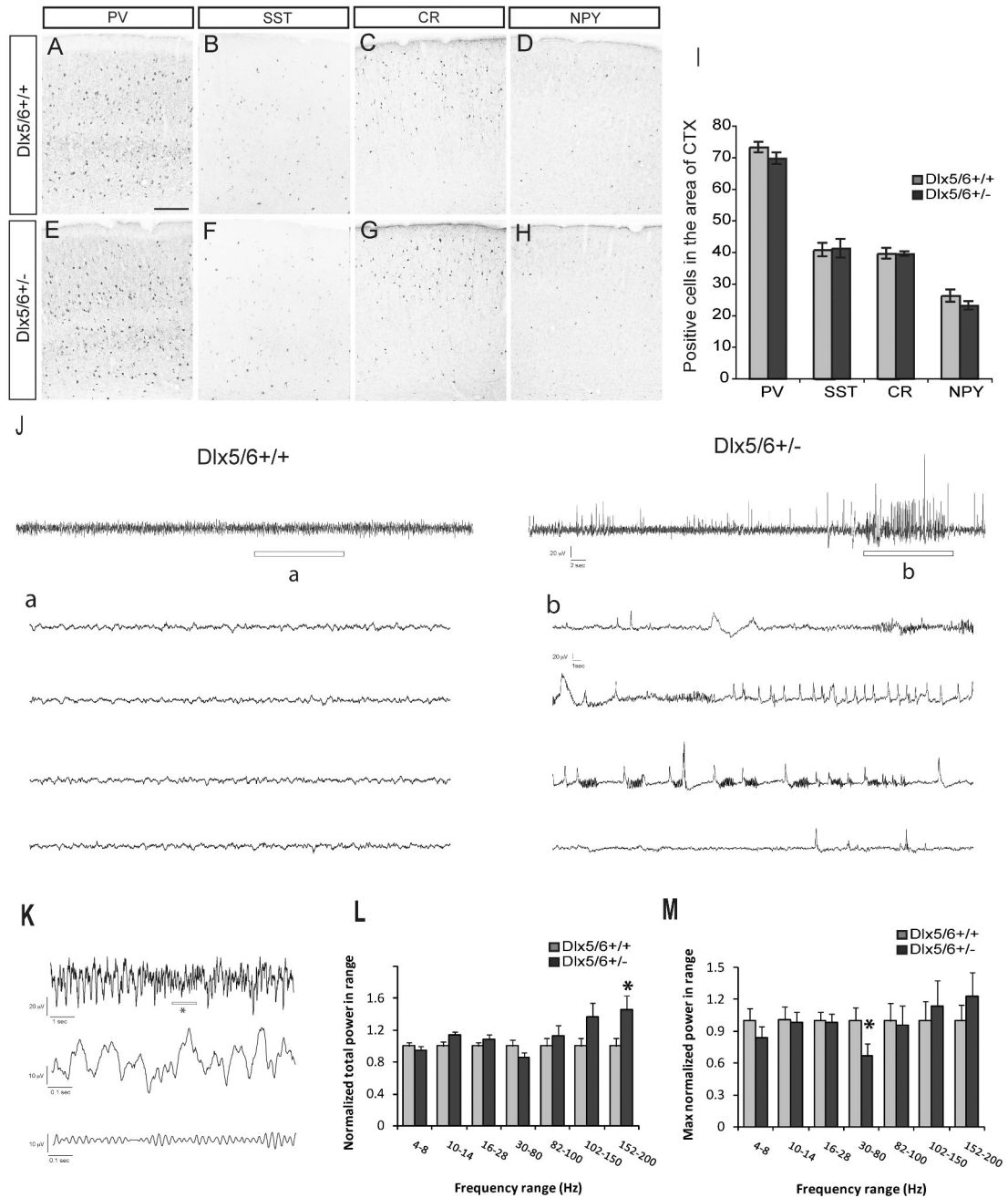


Figure 7. Characterization of GFP expression in adult neocortical interneurons from the *Dlx5* BAC transgenic mouse. (A) GFP immunofluorescence in coronal sections through somatosensory cortex at 2 months of age. (B~E) Double immunofluorescence confocal images with anti-GFP and either anti-PV, anti-SST, anti-NPY or anti-CR antibodies. Quantification of the percentage of GFP⁺ cells that express each of the different interneuron markers (green bar) and the percentage of PV, SST, NPY or CR cells that express GFP (red bar) in layer II-IV (F) and layer V-VI (G). (H) Model of transcription factors that control the development of cortical and hippocampal interneurons. LGE/dCGE are proposed to generate CR/VIP⁺ and a subset of NPY⁺ (late born) interneurons, which express *Dlx1* and require it for their survival. The dorsal MGE generates SST⁺ (including SST/CR⁺ and SST/NPY⁺) interneurons that

express *Dlx1* and *Lhx6*, and require them for their survival and differentiation, respectively. The ventral MGE produces PV⁺ interneurons that express *Dlx5*, and *Lhx6*, and require *Dlx5*, *Dlx6* and *Lhx6* for their differentiation. Abbreviations: LGE: lateral ganglionic eminence; MGE: medial ganglionic eminence; dCGE: dorsal caudal ganglionic eminence; SVZ: subventricular zone; VZ: ventricular zone. Scale bar: 100μm.

**Figure 8.**

Dlx5/6^{+/-} mice show spontaneous electrographic seizures and reduced maximum gamma power in the absence of gross histological abnormalities. (A~H) Expression of PV, SST, CR and NPY in somatosensory cortex of *Dlx5/6^{+/+}* and *Dlx5/6^{+/-}* littermates. (I) Quantification of PV⁺, SST⁺, CR⁺, NPY⁺ cells within a region of 380,000 μ m² of the somatosensory cortex. Scale bar: 200 μ m. (J) Sample EEG traces obtained during daytime recordings from freely moving adult *Dlx5/6^{+/+}* and *Dlx5/6^{+/-}* mice. *Top*: 60-second long EEG recordings. *Bottom*: Enlargement of region indicated by “a” or “b” in the top trace. Note the presence of an abnormal epileptiform-like electrographic discharge in “b”. Scale bars (top): 20 uV, 2 sec; (bottom) 20 uV, 1 sec. (K) Sample EEG traces used for power analysis. *Top*: 10-second long

EEG recording from a *Dlx5/6^{+/+}* mouse. *Middle*: enlargement of region indicated by “*” in the top trace. *Bottom*: Same as middle, but filtered between 30 and 80 Hz. (L) Total power as a function of frequency band for *Dlx5/6^{+/+}* or *Dlx5/6^{+/-}* mice. For each frequency band, total power was normalized by the mean total power in *Dlx5/6^{+/+}* mice. Each bar represents an average over four mice from each group, five 60-second epochs from each mouse, and two EEG recording sites (n = 40 per group). (M) Maximum power within each frequency band for *Dlx5/6^{+/+}* or *Dlx5/6^{+/-}* mice. For each mouse, we selected the 60-second epoch with the most power in each frequency band. Each bar represents an average over four mice from each group, and two EEG recording sites in each mouse (n = 8 per group). * $P < 0.05$ by one-way ANOVA.